Int. J. Nano Dimens. 6(2): 141-151, Spring 2015
ISSN: 2008-8868

Contents list available at **IJND**

International Journal of Nano Dimension

Journal homepage: *www.IJND.ir*

Convective heat transfer enhancement of the Water-based magnetite nanofluids in the presence of a 3-D low-intensity magnetic field

E. Esmaeili[1,*]
R. Ghazanfari[2]
S. Farsad[2]

[1] *Birjand University of Technology, Department of Chemical Engineering, Birjand, Iran.*
[2] *Birjand University of Technology, Department of Mechanical Engineering, Birjand, Iran.*

Received 06 June 2014
Received in revised form
09 August 2014
Accepted 20 August 2014

* Corresponding author:
Elaheh Esmaeili
Birjand University of Technology, Department of Chemical Engineering, P.O. Box 97175/569, Birjand, Iran.
Tel +98 5618821271
Fax +98 561 2252098
Email esmaeili@birjandut.ac.ir

ABSTRACT

In the current investigation, Fe_3O_4 water-based nanofluids were synthesized to examine the effect of an alternative 3-D external magnetic field on its thermal behavioral pattern. A solvothermal method was used to prepare the magnetite nanoparticles. To characterize the nanoparticles, the study employed transmission electron microscopy, X-ray diffraction, Fourier transform infrared spectroscopy, vibrating sample magnetometer and zeta-potential experiments. Vibrating sample magnetometer evaluations thoroughly confirmed the super-paramagnetic characteristics of the nanoparticles. Therefore, exposition of the resulting nanofluids to an AC external magnetic field led to the formation of aligned dipoles parallel to the applied field. Afterwards, the net magnetization in the absence of the external field was set to zero. Thermal measurements demonstrated an enhancement of convective heat transfer coefficients, particularly in the case of more diluted samples. The highest value of h was associated with the most diluted sample, where the h value was two times greater than that in the base fluid at V=1.4 V. This was attributed to the augmentation of both the Brownian motions and the viscosity gradients in the centerline of the test section.

Keywords: *External magnetic field; Convective heat transfer; Nanofluid; Magnetite; Magnetization.*

INTRODUCTION

Nowadays, the efficiency and reliability in many industrial and engineering fields such as automobile building, power generation, aerospace, transportation, and especially, micro-heating systems are significantly associated with their heat transport properties. Conventional heat transfer fluids such as water, ethylene glycol and kerosene show finite heat transfer characteristics. Besides, use of some apparatuses such as fins and the vibration of the heated surfaces restricts many heat transfer applications [1-2].

Choi et al. [1] initially identified a kind of nanofluid which showed a good enhancement of thermal properties and energy efficiency of the base fluid. They defined the term “nanofluid” as the nanoparticles dispersed in the base fluid [3]. Two nanofluid preparation methods are suggested, the first being a single-step method based on which nanofluids are simultaneously synthesized along with the nanoparticles and the second a two–step method in which the nanoparticles are separately prepared, and then, dispersion in the base fluid follows [1, 4].

Recently, ferrofluids have drawn considerable attention thanks to their having both magnetic and fluid characteristics, which in turn, makes them appropriate for interesting applications in various industries. However, a few investigations on the heat transfer properties of the magnetic fluids have been reported [5-7].

Guo et al. [3] synthesized a stable magnetic nanofluid containing γ-Fe_2O_3 nanoparticles through a two-step method to discover the behavioral pattern of these kinds of materials in the enhancement of thermal transport properties. They observed remarkable convective heat transfer coefficients in a laminar flow regime, when they changed the Reynolds number (Re) at various volume fractions. Hong et al. [8] investigated the effect of magnetic field on the thermal conductivities of a water-based nanofluid made of a physical mixture of carbon nanotubes and Fe_2O_3 nanoparticles. They speculated that the formation of aligned chains of Fe_2O_3 particles under the applied magnetic field connects the carbon nanotubes to each other, leading to the enhancement of the thermal conductivity. In another investigation, Philip et al. [9] used a nanofluid consisting of a colloidal suspension of magnetite nanoparticles with an average diameter of 6.7 nm. They could control the linear aggregation length from nano-scales to micro-scales under the influence of the magnetic field. Afterwards, they measured the thermal conductivity enhancements of the nanofluid at ca. 216% by using 4.5 vol. % of nanoparticles. Ganguly and co-workers [10] also numerically studied the heat transfer augmentation induced by several dipoles to identify the changes of the streamlines of the ferrohydrodynamic convection between two plates. However, they applied a two-dimensional magnetic field to evaluate the heat transfer properties of the ferrofluid.

Among the common synthesis methods, including co-precipitation [11-14], ultrasonic-assisted chemical co-precipitation [15], chemical reduction method [16], solvothermal synthesis [17-19], micro-emulsion [20], chemical co-precipitation [21], oxidation of $Fe(OH)_2$ by H_2O_2 [22], and microwave irradiation [23], this paper, in its contribution, used a solvothermal method because of its greater efficiency and homogeneity.

Although a few studies have investigated the external magnetic field, none of them has concentrated on the influence of the magnetic field on the convective heat transfer coefficients (h). In this study, the aim is to examine the effect of an AC three-dimensional magnetic field on Fe_3O_4 water-based nanofluids in order to evaluate the variations of the convective heat transfer coefficients.

EXPERIMENTAL

All the chemicals were purchased from Merck and used as received. To synthesize the Fe_3O_4 nanoparticles, a solvothermal technique was applied [17-19]. Briefly, $FeCl_3.6H_2O$ (0.454 g) was dissolved in 70 cc ethylene glycol, followed by dissolving 3.6 g Polyvinyl Pyrrolidone (PVP). Afterwards, 2.3 g sodium acetate was added to the resulted solution, then, this solution was transferred to a 500 ml Teflon-lined autoclave. The reaction temperature was adjusted at 200^{o}C for 16 h, considering the pressure of the autoclaved solution (around 20 bar). Finally, the remained product was filtered and dried in a vacuum oven at 90°C for 6 h.

The water-based nanofluids were easily produced by a two-step method, basing on the appropriate amounts of Fe_3O_4 nanoparticles were dispersed in the water, followed by sonication. In the present investigation, we used three different concentrations of 0.0025 wt. % (sample 1), 0.005 wt. % (sample 2) and 0.01 wt. % (sample 3) Fe_3O_4 in the preparation of the nanofluids. The experimental apparatus for the investigation of convective heat transfer is presented in Figure 1a and 1b. In general, the experimental set-up consists of a test section made of copper with an inner diameter of 8.65 mm and the length of 1.2 m, a pump supplied by a digital flow controller, a reservoir tank, a circulator and some stators which establish the magnetic field. An electrical element was used to heat up the test section during the experiment. In this research, the constant heat flux was considered to be ca. 200 W, and the test section was insulated thermally to minimize the heat loss from the tube to the ambient. In addition to the inserting of two thermocouples in the middle of cross sections of tube for the inlet and outlet fluids of the test section, we soldered five thermocouples in the increments of 20 cm on the copper tube wall.

To adjust the Re number in the desired amounts, we installed a digital flow controller connected to the pump. A circulating system was also used to preserve a constant temperature at the inlet of the test section.

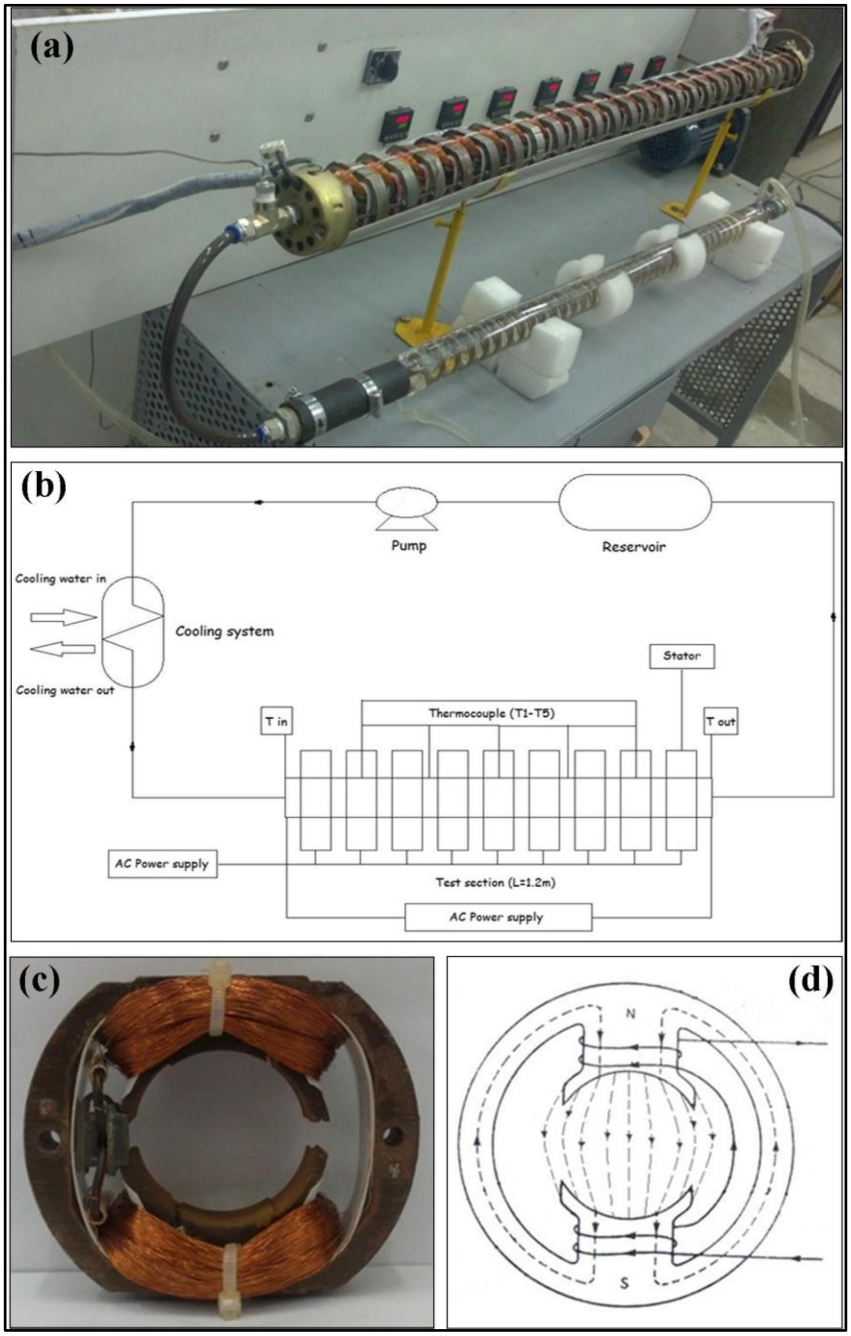

Fig. 1. a) The experimental apparatus used for the examination of the forced convective heat transfer characteristics, b) a schematic representation of the experimental set-up, c) a stator acting as the field magnet, d) the field lines produced by the stators.

To calculate the convective heat transfer coefficients of the nanofluids, in addition to measuring the experimental constant heat flux (q''), the wall temperatures along the copper tube, mean temperature of the bulk fluid and flow rate are also required [4]. Then,

$$h(x) = \frac{q''}{T_s(x) - T_m(x)},$$

$$\text{where} \quad T_m(x) = T_{m,i} + \frac{q'' P}{\dot{m} C_p} \qquad \text{Eq. (1)}$$

where, $T_m(x)$, $T_s(x)$ and $h(x)$ are the mean temperature of fluid, the wall temperature of tube and the heat transfer coefficient, respectively. The aim of the measurements is to obtain the average heat transfer coefficient (h_{ave}) of the nanofluids.

In order to investigate the effect of an external magnetic field, a low- voltage three-dimensional magnetic field perpendicular to the fluid's flow was developed, as demonstrated in Figure 1c and 1d. Controlling the strength of the magnetic field was conducted by an AC power supply ranging from 0 V up to about 5 V which exerts a voltage difference to both ends of the test section.

The thermal conductivity (k) of the nanofluids was measured at 20°C by using a KD2 thermal property meter (Lab cell Ltd, UK), which worked on the basis of the transient hot wire method. Zeta potential value was performed by a Malvern ZS analyzer (Malvern Instrument Inc, London, UK) to determine the dispersion behavior of the nanofluid. Transmission electron microscopy images were obtained using a CM-FEG-Philips, supplied by an accelerating voltage of 120 keV to investigate the dispersion and the metal particle size of the magnetite (Fe_3O_4) nanoparticles. X-ray diffraction with Cu Kα radiation source (Philips PW-1840) was applied to study the crystalline phases of the catalysts. Fourier transform infrared (Bruker, Vertex 70) was employed to indicate the chemical nature of the magnetite nanoparticles. Also, to characterize the magnetic properties of the Fe_3O_4 nanoparticles, the vibrating sample magnetometer (Lake Shore 7400) system was used.

RESULTS AND DISCUSSION

Figure 2a and 2b show the Transmission electron microscopy images of Fe_3O_4 nanoparticles synthesized via solvothermal method, having porous structures. The presented photographs confirmed that the synthesis technique leads to the well-dispersed particles, mostly in the range of about 60-80 nm in accordance with the histogram implied in Figure 2c. According to Figure 2d, the zeta potential value of around 23 mV indicates that the electrostatic repulsion is relatively sufficient for a good stabilization of the nanoparticles, the same as what is found in the literature [24-25].

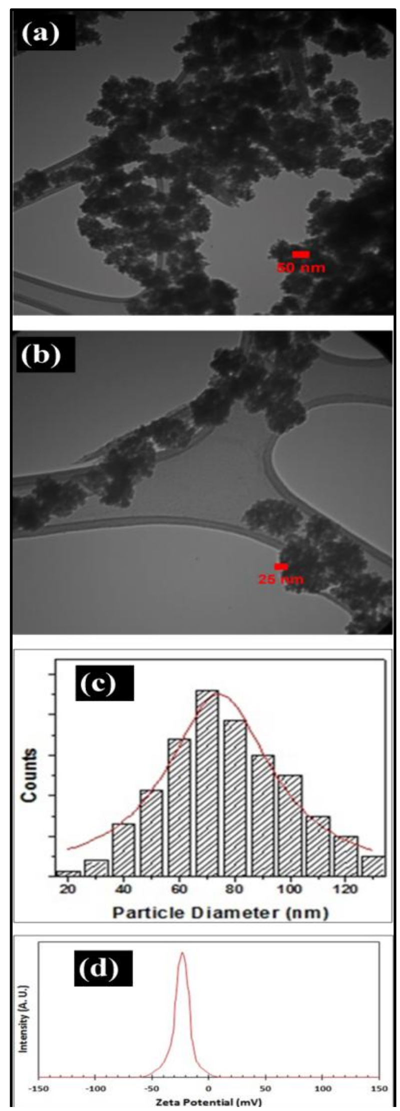

Fig. 2. Transmission electron microscopy photographs of Fe_3O_4 nanoparticles (a and b), the histogram of nanoparticles diameters of Fe_3O_4 (c) and the zeta potential of Fe_3O_4 nanoparticles (d).

The x-ray diffraction pattern of Fe_3O_4 nanoparticles is shown in Figure 3. According to this illustration, the crystallite planes of 220, 311, 400, 422, 511, 440, 620 and 622 correspond to the Bragg angles of about 30.3°, 35.6°, 43.2°, 53.6°, 57.2°, 62.8°, 71.8° and 74.2°, respectively, indicating the crystalline nature of Fe_3O_4 nanoparticles [11-12, 15]. Crystallite size measurements were determined from the full-width at half maximum (FWHM) of the strongest reflection of the (311) peak, using the Scherrer approximation, which assumes the small crystallite size to be the cause of line broadening.

$$D = \frac{k\lambda}{\beta cos\theta} \qquad Eq.(2)$$

Where D is the crystallite mean size, k is a shape function for which a value of 0.9 is used, l.54 nm is the wavelength of the radiation, β the full-width at half maximum (FWHM) in radians, and θ the Bragg angle. The average crystallite size of the magnetite nanoparticles resulted from Scherrer's equation [26] was found to be around 6 nm, which differs so much from those displayed in Figure 2. This confirms that the Fe_3O_4 nanoparticles shown in Figure 2 are composed of 6-nm nanoparticles, which finally form the porous structures.

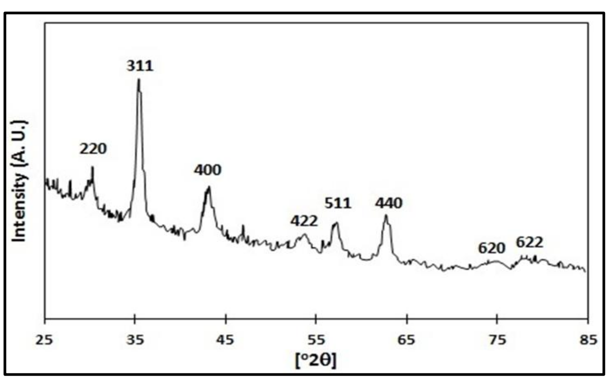

Fig. 3. X-ray diffraction pattern of Fe_3O_4 nanoparticles.

Figure 4 presents the Fourier transform infrared spectrum of Fe_3O_4 nanoparticles prepared by solvothermal method. The peaks observed at 457 up to 430 cm^{-1} are associated with the characteristic peaks of Fe-O stretching vibrations. The presence of Fe_3O_4 nanoparticles is strongly supported by a peak centered at 580 cm^{-1} [16, 27]. Some other peaks may be attributed to some impurities due to decomposition of sodium acetate and/or Polyvinyl Pyrrolidone (PVP) applied in the synthesis procedure. For instance, the peaks appeared at the vibration wavelengths of 1276, 1663 and ca. 2850-2950 cm^{-1} may be assigned to the C-C, C=O stretching bands and methyl groups associated with decomposition of sodium acetate, respectively [28-29]. Furthermore, the peaks centroid at around 1060 cm^{-1} and 3200-3400 cm^{-1} are characteristically indicative of the stretching vibration modes of CH-OH and/ or OH and NH_2 groups [13], correspondingly, as shown in Figure 4.

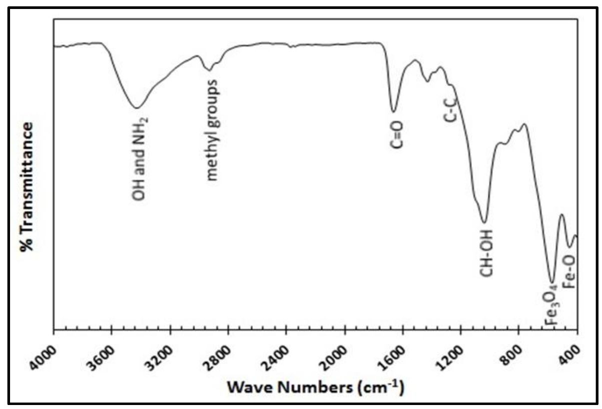

Fig. 4. Fourier transform infrared spectroscopy of Fe_3O_4 nanoparticles synthesized by solvothermal technique.

A field-dependent magnetization curve M (H) at room temperature is displayed in Figure 5a. The saturation magnetization is found to be ca. 63.6 emu g^{-1} at room temperature, which is slightly smaller than the bulk value; i.e. 92 emu g^{-1} [17]. Since there is negligible coercivity in the magnetization curve with no hysteresis loop, one may find that the Fe_3O_4 nanoparticles have superparamagnetic characteristics [30]. For such systems, the magnetic moments of the particles are free to rotate in response to any applied magnetic field [27]. Therefore, one may expect that exposing the resulting nanofluids in the current investigation to any external magnetic field leads to the formation of aligned dipoles parallel to the applied field, and, afterwards, the net magnetization in the absence of the external field is equal to zero [14, 31-32]. Figure 5b demonstrates the highly potential magnetic characteristics of the magnetite in the presence of an external magnetic field.

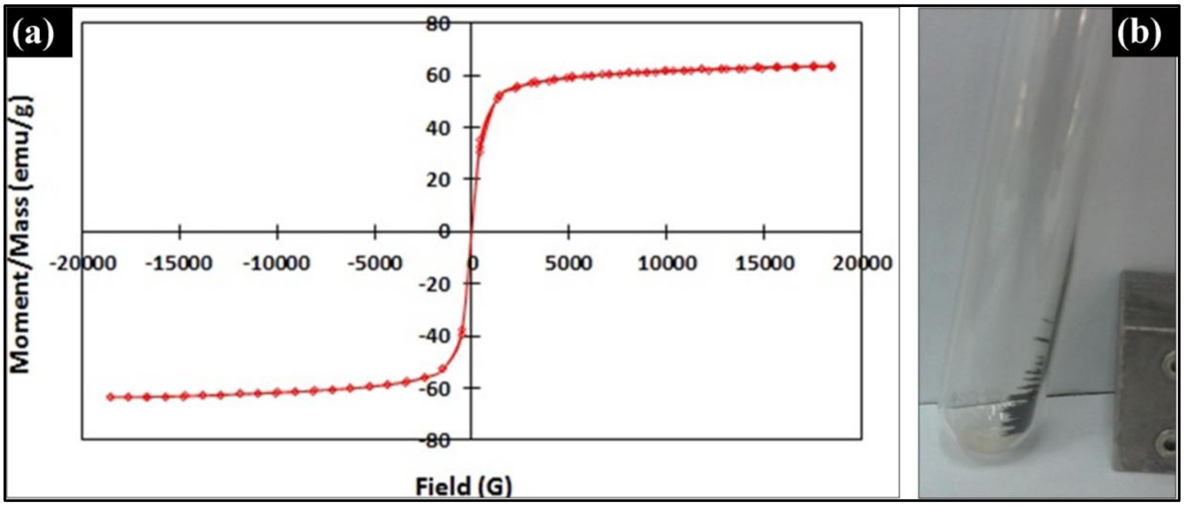

Fig. 5. a) Field-dependent magnetization curve of magnetite nanoparticles at room temperature, b) The magnetic behavior of Fe_3O_4 nanoparticles in the presence of an external magnet.

Heat conductivity measurements show almost similar values for all the three examined nanofluids; however, the results present a slight enhancement of the effective thermal conductivity values with the increase in the concentration of Fe_3O_4 in the nanofluids. Thermal conductivity measurements of all the samples are found to be ca. 15-17 % more than the base fluid. Paul et al. [1] reached up to 48% enhancement in thermal conductivities at 0.00026 vol. % concentration and 21 nm average particle sizes. According to them, the significant enhancement in thermal conductivity of the nanofluids at low concentrations may be attributed to the porous features of the nanoparticles.

Figure 6 illustrates the relative heat transfer coefficients (h_r), where h_r is defined as the resulting amount of $h_{nanofluid}$ (heat transfer coefficient of the nanofluid) divided by h_{water} (heat transfer coefficient of water). According to Figure 6, in the absence of the external magnetic field (i.e. V=0), when the nanofluid is more concentrated, one observes an augmentation in h_r. Therefore, the highest h_r belongs to sample 3, i.e. ca. 1.7, compared with the other samples. Considering low concentrated nanofluids as well as low values of effective heat conductivities, one may find that the h enhancement values are more pronounced. Paul et al. [1] suggested that at very low concentrations, some combined effects such as high, specific surface area and the Brownian motions of the particles may be responsible for the heat transfer enhancement, and then, the improvement mechanisms are not the same as what was observed for high concentrated nanofluids. In the current investigation, the porous structures of the Fe_3O_4 nanoparticles (as shown in Figure 2), particularly along with the Brownian motions of the nanoparticles, may rationalize the enhanced convective heat transfer.

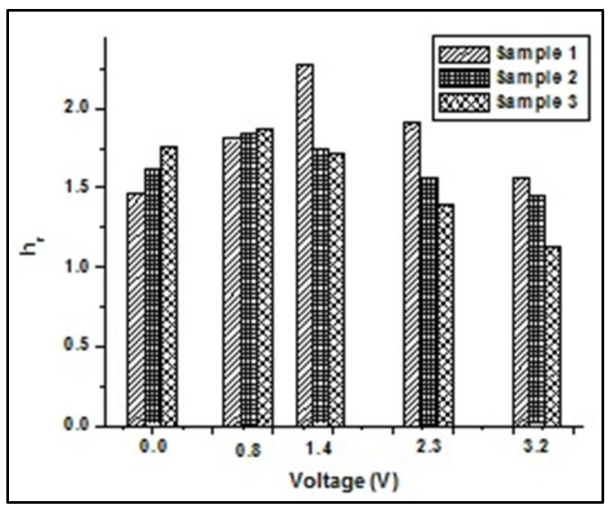

Fig. 6. The results of relative heat transfer coefficients (h_r) of the nanofluids with the variation of the magnetic field strength.

Figure 6 demonstrates that enhancement of h_r is caused by the increase in the magnetic field strength, particularly in the case of sample 1, which owns the lowest concentrations. Therefore, according to Figure 6, the highest value of h_r is found to be ca. two times that of the water, when it works under the voltage of around 1.4 V. This enhanced measurement confirms the positive effect of an external magnetic field, particularly in the case of more diluted nanofluids. To the best of our knowledge, an external magnetic field could easily align the dipoles of any paramagnetic material along the applied field [31]. Therefore, following the exertion of the magnetic field to both ends of the test section, the nanoparticles get align in the direction of the resulting field, i.e. perpendicular to the fluid's flow which was considered to be horizontally.

So far, many interesting factors such as various effects of thermal conductivities under static and dynamic conditions, energy transfer by nanoparticles dispersion, particle migration due to viscosity gradient, non-uniform shear rate, Brownian diffusion and thermophoresis were assumed as having an impact on the enhancement of the convective heat transfer coefficient [32-36]. However, Xuan and Li [33] suggested that highly dispersed nanoparticles could flatten the temperature distribution, which will in turn; augment the heat transfer rate between the fluid and the wall. Wen and Ding [34] numerically showed that the particle migration induced by the viscosity gradient and then, by a non-uniform shear rate leads to a higher heat transfer coefficient of nanofluids. Buongiorno [35] also theoretically confirmed the effect of nanoparticle dispersion on the energy transfer of nanofluids and conclusively, showed that energy transfer by nanoparticle dispersion is negligible. Therefore, according to Wen and Ding [36], particle migration leads to a considerable radial non-uniformity in particle concentration, affecting the local thermal conductivity and viscosity. In the current investigation, exerting an external magnetic field composed of 3-D dipoles, surrounding the test section, results in the transverse movements of nanoparticles (see the field lines in Figure 1d), as inferred from Eq. (3).

$$\vec{F} = q\vec{V} \times \vec{B} \qquad \text{Eq. (3)}$$

As a consequence of using the alternative current field, one may expect the sweeping motions across the tube cross-section. Then, higher viscosity of nanoparticles near the centerline of the copper tube is expected, which, in turn, flattens the velocity profile, and, therefore, decreases the difference between the tube wall temperature and bulk mean temperature of nanofluids [37].

According to the above-mentioned explanations, because of the use of an AC power supply to produce a 3-D magnetic field, worm-like movements are expected for the nanoparticles. In fact, in addition to the intrinsic Brownian motions of the particles, due to the presence of an external magnetic field, extra movements exist too. In other words, we succeeded to make more contacts between nanoparticles along with the increment of viscosity gradient in the centerline of the test section, which could develop the thermal properties of the nanofluids.

According to Figure 6, maximum values of h_r for all of the samples are followed by a suddenly decreasing tendency. Taking into account the high concentration of nanoparticles in the centerline of the tube, it is obvious that the increase in the magnetic field strength together with the augmentation of the contacts between the nanoparticles leads to the flocculation of the nanoparticles, decreasing the convective heat transfer properties. According to Figure 6, one may observe that the decreasing propensity of the h_r values is more significant for sample 3 which contains the highest concentration. For instance, h_r reaches up to 1.12 times of the base fluid at V=3.2 V, which is even lower than h_r=1.7 in the absence of the external magnetic field. This confirms the clumping of the nanoparticles together under the influence of more intensified magnetic fields.

Fig. 7 implies the effect of magnetic field strength on the convective heat transfer coefficient (h) of the nanofluids, when Re number is varied. Zabihi and co-workers [2] stated that in higher Re numbers, the effect of Brownian motion of nanoparticles and, then, the amount of h enhancement increases. Buongiorno [35] showed that the Brownian diffusion and thermophoresis effects are significant mechanisms for considerable variations in viscosity and thermal conductivity of nanofluids within the laminar sublayer of the turbulent boundary layer; however, turbulent boundary layers include greater mixing compared with laminar boundary layers [38]. Since, the Brownian Motions and the aggregation of nanoparticles have two contrary effects on the h variations; the important subject in this course is which one of them is prevailing.

Figure 7 shows that the h variations are influenced by the changes in the magnetic field strength. According to Figure 7, an increasing tendency for the h values of the Fe_3O_4 water-based nanofluid is observed, when the voltage of the magnetic field is varied within the range of 0-1.4 V. Based on the results, in this voltage range, the h values increase from 1550 up to 2550 W/m^2K. At Re=1395, because of having a laminar flow as well as the absence of eddy convection, one may find that the use of an AC magnetic field results in particle migration, mostly to the centerline of the tube. According to what illustrated in Figure 7, the amount of h enhancements is insignificant in the Re number of 2335 compared to those resulting at Re=1395, even after applying the magnetic field. This may be attributed to the transition state from laminar to turbulent flow, having complex concepts of boundary layers which are not clearly known yet; i.e. unspecified changes of the boundary layer thickness may be responsible for this observation.

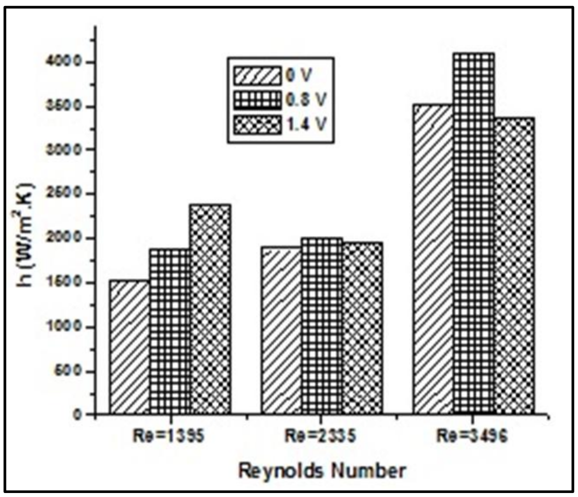

Fig. 7. The h values of nanofluids at different Re numbers with varying magnetic field strengths.

According to Figure 7, the resulting measurements show a considerable h enhancement at Re=3496. Considering the increase of turbulency and the formation of eddies, one may conclude that the eddy convection is an important factor along with the increase of viscosity gradient induced by the external magnetic field to enhance the forced-convective heat transfer properties. However, the increase in the magnetic field strength up to V=1.4 V leads to the cutting back on the value lower than that in the absence of magnetic field. This indicates that the effect of flocculation of nanoparticles is prevailing as a conclusion of both the eddy convection and the particles motions induced by the applied field.

In general, the suggested mechanism rationalized in this contribution is in good agreement with the literature [37]; however, the presentation of an exact approach to show the effect of a 3-D magnetic field on the forced-convective heat transfer characteristics requires more experiments.

CONCLUSIONS

In this investigation, we synthesized the porous superparamagnetic Fe_3O_4 nanoparticles with an average particle size of 75 nm through a potential solvothermal method in order to investigate the influence of a 3-D low voltage magnetic field on the convective heat transfer measurements. According to the results, use of the magnetic field had a significant effect on the h values induced by both Brownian motions and viscosity gradients; however, this enhancement was strongly sensitive to the applied field strength. Since, exerting an AC magnetic field led to the augmentation in contacts between particles, the coagulation of the particles was expected. Conclusively, these findings showed promising insights into the enhancement of the forced-convective heat transfer properties of nanofluids by applying an appropriate magnetic field.

ACKNOWLEDGEMENTS

First of all, the authors would like to express their gratitude for the financial supports of Iran National Science Foundation (INSF) with project number 91058848. Also, we wish to thank Dr. Alimorad Rashidi, head of Nanotechnology Research Center at RIPI for his scientific helps.

REFERENCES

[1] Paul G., Pal T., Manna I., (2010), Thermo-physical property measurement of nano-gold dispersed water based nanofluids prepared by chemical precipitation technique. *J. Colloid Interface Sci*. 349: 434–437.

[2] Zabihi K., Gholamian F., Vasefi S., (2013), Experimental and numerical investigation of Al2O3-water nanofluid inside a triangular tube. *World Appl. Sci. J.* 22: 601-607.

[3] Guo S., Li Y., Jiang J., Xie H., (2010), Nanofluids containing γ-Fe2O3 nanoparticles and their heat transfer enhancements. *Nanoscale Res. Lett*. 5: 1222–1227.

[4] Amrollahi A., Rashidi A., Lotfi R., Emami Meibodi M., Kashefi K., (2010), Convection heat transfer of functionalized MWNT in aqueous fluids in laminar and turbulent flow at the entrance region. *Int. Commun. Heat Mass Tran*. 37: 717–723.

[5] Bhimani Z., Wilson B., (1997), New low cost ferrofluidic sealing challenges the mechanical seal. *Ind. Lubr. Tribol*. 49: 288-290.

[6] Jiang J., Gan Z., Yang Y., Du B., Qian M., Zhang P., (2009), A novel magnetic fluid based on starch-coated magnetite nanoparticles functionalized with homing peptide. *J. Nanopart. Res*. 11: 1321-1330.

[7] Yang Y., Jiang J., Du B., Gan Z., Qian M., Zhang P., (2009), Preparation and properties of a novel drug delivery system with both magnetic and biomolecular targeting. *J. Mater. Sci. Mater. Med*. 20: 301-307.

[8] Hong H., Wright B., Wensel J., Jin S., Ye X., Roy W., (2007), Enhanced thermal conductivity by the magnetic field in heat transfer nanofluids containing carbon nanotube. *Synthetic Met*. 157: 437–440.

[9] Philip J., Shima P., Raj B., (2008), Evidence for enhanced thermal conduction through percolating structures in nanofluids. *Nanotechnol.* 19: 305706-305711.

[10] Ganguly R., Sen S., Puri I., (2004), Heat transfer augmentation using a magnetic fluid under the influence of a line dipole. *J. Magn. Magn. Mater*. 271: 63–73.

[11] Ghandoor H., Zidan H., Khalil M., Ismail M., (2012), Synthesis and some physical properties of magnetite (Fe3O4) nanoparticles. *Int. J. Electrochem. Sci.* 7: 5734 – 5745.

[12] Sun J., Zhou S., Hou P., Yang Y., Weng J., Li X. et al., (2007), Synthesis and characterization of biocompatible Fe3O4 nanoparticles. *J. Biomed. Mater. Res*. 80: 333-341.

[13] Kaushik A., Khan R., Solanki P., Pandey P., Alam J., Ahmad S. et al., (2008), Iron oxide nanoparticles–chitosan composite based glucose biosensor. Biosens. *Bioelectron*. 24: 676–683.

[14] Lopez J., González F., Bonilla F., Zambrano G., Gómez M., (2010), Synthesis and characterization of Fe3O4 magnetic nanofluid. *Rev. Lat. Am. Metal. Mater.* 30: 60-66.

[15] Wu S., Sun A., Zhai F., Wang J., Xu W., Zhang Q. et al., (2011), Fe3O4 magnetic nanoparticles synthesis from tailings by ultrasonic chemical co-precipitation. *Mater. Lett*. 65: 1882–1884.

[16] Ankamwar B., Thorar A., (2013), Rod-shaped magnetite nano/microparticles synthesis at ambient temperature. *J. Chem.* 1: 1-6.

[17] Sun Q., Ren Z., Wang R., Chen W., Chen C., (2011), Magnetite hollow spheres: solution synthesis, phase formation and

magnetic property. *J. Nanopart. Res*. 13: 213–220.

[18] Zhang Q., Zhu M., Zhang Q., Li Y., Wang H., (2009), The formation of magnetite nanoparticles on the sidewalls of multi-walled carbon nanotubes. *Compos. Sci. Technol.* 69: 633–638.

[19] Zhang Z., Kong J., (2011), Novel magnetic Fe3O4/C nanoparticles as adsorbents for removal of organic dyes from aqueous solution. *J. Hazard. Mater*. 193: 325–329.

[20] Zhang D., Tong Z., Li S., Zhang X., Ying A., (2008), Fabrication and characterization of hollow Fe_3O_4 nanospheres in a microemulsion. *Mater. Lett*. 62: 4053–4055.

[21] Jiang W., Yang H., Yang S., Horng H., Hung J., Chen Y., (2004), Preparation and properties of superparamagnetic nanoparticles with narrow size distribution and biocompatible. *J. Magn. Magn. Mater*. 283: 210–214.

[22] Yu L., Zheng L., Yang J., (2000), Study of preparation and properties on magnetization and stability for ferromagnetic fluids. *Mater. Chem. Phys*. 66: 6–9.

[23] Khollam Y., Dhage S., Potdar S., (2002), Microwave hydrothermal preparation of submicron-sized spherical magnetite (Fe3O4) powders. *Materer. Lett*. 56: 571–577.

[24] Mahendran V., Philip J., (2013), An optical technique for fast and ultrasensitive detection of ammonia using magnetic nanofluids. *Appl. Phys. Lett*. 102: 063107.

[25] White B., Banerjee S., O'Brien S., Turro N., Herman I., (2007), Zeta-potential measurements of surfactant-wrapped individual single-walled carbon nanotubes. *J. Phys. Chem*. 111: 13684-13690.

[26] Waje S., Hashim M., Yusoff W., Abbas Z., (2010), X-ray diffraction studies on crystallite size evolution of CoFe2O4 nanoparticles prepared using mechanical alloying and sintering. *Appl. Surf. Sci*. 256: 3122–3127.

[27] Nan A., Craciunescu I., Turcu R., (1999), Aspects on Fundaments and Applications of Conducting Polymers: *A Practical Approach, Kluwer Academic Publishers*, Chapter 8, 159-182.

[28] Ibrahim M., Nada A., Kamal D., (2005), Density functional theory and Fourier transform infrared spectroscopic study of carboxyl group. *Indian J. Pure Ap. Phy*. 43: 911-917.

[29] Esmaeili E., Rashidi A., Khodadadi A., Mortazavi Y., Rashidzadeh M., (2014), Palladium–Tin nanocatalysts in high concentration acetylene hydrogenation: A novel deactivation mechanism, *Fuel Process. Technol.* 120: 113–122.

[30] Lu A., Salabas E., Schuth F., (2007), Magnetic nanoparticles: synthesis, protection, functionalization, and application. *Angew. Chem. Int. Edit*. 46: 1222–1244.

[31] Kumar A., (2010), Synthesis and characterization of manganese zinc ferrite, M.S. Thesis, Thapar University, Patiala.

[32] Nandwana V., Elkins K., Poudyal N., Chaubey G., Yano K., Liu J., (2007), Size and Shape Control of Monodisperse FePt Nanoparticles. *J. Phys. Chem. C* 111: 4185-4189.

[33] Xuan Y., Li Q., (2003), Investigation on convective heat transfer and flow features of nanofluids. *ASME J. Heat Tran*. 125: 151–155.

[34] Wen D., Ding Y., (2005), Effect on heat transfer of particle migration in suspensions of nanoparticles flowing

through minichannels. *Microfluid. Nanofluidics*. 1: 183–189.

[35] Buongiorno J., (2006), Convective transport in nanofluids. *ASME J. Heat Tran*. 128: 240–250.

[36] Wen D., Ding Y., (2004), Experimental investigation into convective heat transfer of nanofluids at the entrance region under laminar flow conditions. *Int. J. Heat Mass Tran*. 47: 5181–5188.

[37] Hwang K., Jang S., Choi S., (2009), Flow and convective heat transfer characteristics of water-based Al2O3 nanofluids in fully developed laminar flow regime. *Int. J. Heat Mass Tran*. 52: 193–199.

[38] Taylor R., Coulombe S., Otanicar T., Phelan P., Gunawan A., Lv W. et al.,(2012), Critical review of the novel applications and uses of nanofluids. Proceedings of the ASME 2012 3rd Micro/Nanoscale Heat Mass Tran. *Int. Conf*. 1-16.

Cite this article as: E. Esmaeili *et al.*: Convective heat transfer enhancement of the water-based magnetite nanofluids in the presence of a 3-D low-intensity magnetic field.
Int. J. Nano Dimens. 6(2): 141-151, Spring 2015.